# Photovoltaic heterostructure devices made of sequentially adsorbed poly(phenylene vinylene) and functionalized $C_{60}$

H. Mattoussi[a] and M. F. Rubner
*Center for Materials Science and Engineering, Massachusetts Institute of Technology, Cambridge, Massachusetts 02139*

F. Zhou, J. Kumar, and S. K. Tripathy
*Center for Advanced Materials, University of Massachusetts, Lowell, Massachusetts 01854*

L. Y. Chiang
*National Taiwan University, Taipei, Taiwan*

(Received 20 March 2000; accepted for publication 11 July 2000)

We report on the preparation and characterization of rectifying photovoltaic heterostructure devices made of poly(phenylene vinylene), PPV, and $C_{60}$. The heterojunctions were built from solution using the technique of layer-by-layer sequential adsorption. This technique permits one to control the heterostructure at the molecular scale. Upon illumination with a laser beam, the devices showed large photoresponses (current and voltage) that resulted from a photoinduced electron transfer between the PPV (donor layer) and the $C_{60}$ (acceptor layer). The photocurrent was found to increase with the laser power and with the photon energy of the incident radiation. Also, a constant high photovoltage response of ~700–800 mV was measured. Analysis of the time dependence of the photocurrent rise and decay, when the device was illuminated with a modulated square wave signal (chopped laser beam), permitted us to draw an analogy between the present heterojunction and a circuit made of a capacitor and a resistance in series. © *2000 American Institute of Physics.* [S0003-6951(00)03236-8]

Fast (~picosecond) electron transfer between a semiconducting polymer and buckminster fullerence ($C_{60}$) has been demonstrated.[1–6] In particular, a study of the photoinduced electron transfer between poly[2-methoxy,5-(2-ethylhexyloxy)-1,4-phenylene-vinylene], MEH–PPV, and $C_{60}$ in a heterojunction was reported.[4] In this device, MEH–PPV and $C_{60}$ served as the electron donor and acceptor, respectively. High rectification ratios ($r \sim 10^4$) and large photoresponses (both current and voltage) were reported for MEH–PPV/$C_{60}$ heterostructure devices.[4]

In the present study, we expand the earlier concepts and use the technique of layer-by-layer sequential adsorption to fabricate heterostructure devices made of poly(phenylene vinylene), PPV, and $C_{60}$. In these samples the structures are bilayer-blocks made of PPV/poly(acrylic acid) (PAA) and $C_{60}$/poly(allyl amine hydrochloride) (PAH), which serve as the electron donor and electron acceptor, respectively. Because the films are controlled at the molecular scale (nanometer size), this approach permits one to fabricate various structures, such as two-layer devices with various PPV and $C_{60}$ layer thickness, fully mixed structures, as well as interpenetrating multilayer structures. The approach of layer-by-layer sequential adsorption has been applied to making organic and hybrid organic/inorganic light emitting devices.[7–10] The materials were processed from deionized water solutions. The PPV structure was processed in its charged nonconjugated form, poly(xylylene tetrahydrothiophenium chloride), known as the precursor PPV (or pPPV). This structure was made of alternating individually adsorbed monolayers of pPPV (positively charged) and PAA (negatively charged). The electron acceptor layer was made of alternating monolayers of sulfonated $C_{60}$ (negatively charged) and PAH (positively charged).[11] The pPPV with $M_w \cong 8 \times 10^5$ daltons, was purchased from Lark Enterprise (Bedford, MA) as a solution of about 1%(wt) polymer concentration in water.[12,13] PAA with $M_w \cong 3 \times 10^4$ and PAH with $M_w \cong 10^5$ were purchased as powders from Polysciences Inc. The polymer concentrations were: $10^{-2}$ M/l for solutions of PAA and PAH, ~0.1–0.5%(wt) for pPPV, and ~0.03 M/l was used for $C_{60}$. No counterion excess was added to the solutions. The *p*H was adjusted to ~4.5 for solutions of pPPV, PAH and $C_{60}$, whereas its value was ~3.5 for PAA. The multilayers were built on glass slides with patterned indium tin oxide (ITO) (2000-Å-thick stripes). A computer controlled glass stainer (from Zeiss) was used to carry out the deposition.[7–9] The films were dried for ~12 h in a desiccator, followed by ~12 h in vacuum. They were then heated under dynamic vacuum (at $\sim 10^{-3}$ Torr) for ~10–12 h at 230 °C. This converts the precursor into the final conjugated PPV.[7–10] Aluminum electrodes were evaporated (4 stripes, 2000-Å-thick each) orthogonal to the ITO. This provided several cells that could be addressed individually.

The devices were excited at three different wavelengths $\lambda = 457$, 488, and 514 nm. Measurements of the dark current (no incident light) and photocurrent (device exposed to the laser beam) versus applied voltage were carried out in inert atmosphere ($N_2$). The voltage source (Keithley 230) had its positive contact connected to the ITO and the negative contact connected to the Al electrode (forward bias). The current was measured on a digital multimeter (Hewlett-Packard

[a]Present address: Naval Research Laboratory, Optical Sciences Division, Washington, DC 20375; electronic mail: hedimat@ccs.nrl.navy.mil

 

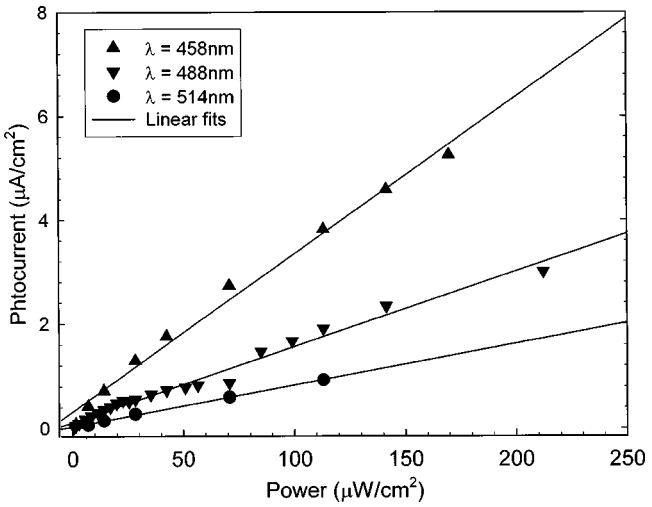


FIG. 1. Photocurrent responses measured for the two-layer devices $[PPV/PAA)_{20}/(C_{60}/PAH)_{60}]$ vs laser power at three wavelengths, $\lambda=514$, 488, and 457 nm. Similar data were measured for 70 and 90 bilayers of $C_{60}$/PAH. Slightly smaller values were measured for 50 bilayers.

34401A). When measuring current–voltage–light power output ($I-V-L$) characteristics, a Si photodiode was used to collect the light emission.[7–10] The voltage was ramped up or down, as a positive or negative bias, in discrete steps, with the current and power output measured at each step.

Figure 1 shows the photocurrent response as a function of the laser power, at zero voltage, for a two-layer device made of 20 bilayers of PPV/PAA and 60 bilayers of $C_{60}$/PAH. The photocurrent response varies linearly with the incident light power at each wavelength. In addition, the slope of each line increases with decreasing wavelength (increasing photon energy). All three curves converge to zero when the incident power is decreased to zero. Figure 2 shows the $I-V$ characteristics for the above device without (dark current) and with laser illumination at $\lambda=488$ nm. The dark current data indicate that the present heterostructure devices have a rectifying behavior, with only small values measured in the forward bias. Upon irradiation, the current increases substantially both in the forward and in the reverse bias. The

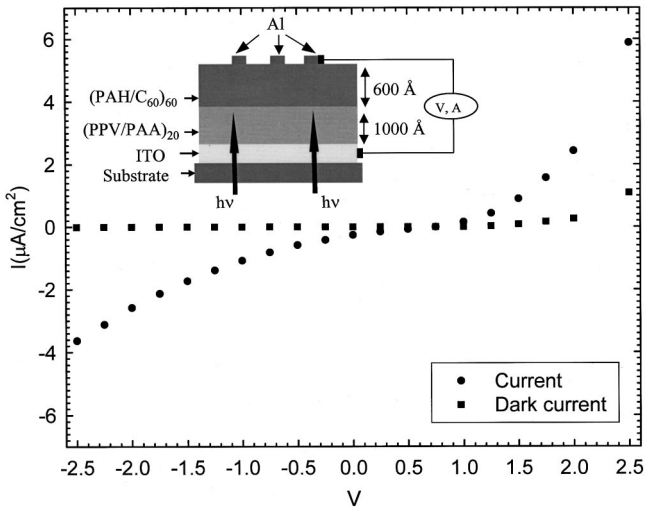


FIG. 2. Photocurrent and dark current vs applied voltage for a heterostructure device $[PPV_{20}/(C_{60})_{60}]$. A laser power of ~14 (mW/cm$^2$) was used. The insert shows the device structure.

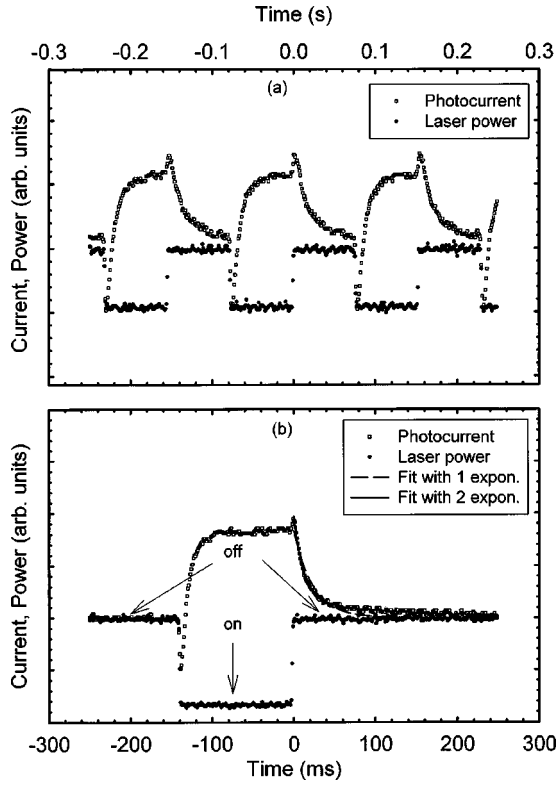


FIG. 3. (a) Time dependence of the photocurrent response for a square wave laser excitation for several periods. (b) Time dependence of the photocurrent for a single stretched period, i.e., longer on and off times for the laser exposure.

$I-V-L$ characteristics of the above devices showed no indication of light emission at voltages up to 15 V. Only a very small emission (<1 cd/m$^2$) could be detected when $V$ exceeded 15 V, but device failure often occurred at such high voltages. Recently, white light emission was reported using single layer devices made of a blend of poly(9-vinylcarbazole), an electron-transport material 2,5-bis-(4-naphthyl)-1,3,4-oxadiazole, and a $C_{60}$ adduct, Th-hexapyrrolidine (THP).[14] THP is a modified fullerene designed to generate radiative emission.

The open circuit voltage response $\Delta V$ measured using an Al cathode is ~700–800 mV. It is not affected by the electron acceptor layer thickness for the present heterostructures.

In an independent experiment, we measured the time dependence of the photocurrent response when the device was exposed to a modulated laser power (square wave incident signal, see Fig. 3). The data shown in Fig. 3(b) for a single period indicate that when the laser beam is turned on, a very rapid increase in the photocurrent (from zero) immediately follows, after which it slowly approaches its asymptotic limit, $I_0$. When the laser power is turned off, the photocurrent decays rapidly from its maximum value, $I_0$, and then asymptotically reaches 0 (its limit at longer time). In addition, the data in Fig. 3 show two transient features (dips and spikes) at the onset and cutoff of the laser power, respectively. Those features are reduced when longer on and off times are used [Fig. 3(b)]. Discarding the two transient processes, the time dependence of the photocurrent can be best fit to two exponential functions

$$I(t)=I_0e^{-t/\tau_{\text{off}}}+I_1e^{-t/\tau_1} \quad \text{for the current decay,}$$

and

$I(t)=I_0(1-e^{-t/\tau_{on}})+I_2(1-e^{-t/\tau_2})$ for the current rise.

In both cases, the fit is dominated by its first term, i.e., $I_0 \gg I_1, I_2$ and $\tau_{on}^{-1} \sim \tau_{off}^{-1} \cong \tau_0^{-1} \gg \tau_1^{-1}, \tau_2^{-1}$. A single exponential curve [e.g., $I(t)=I_0 \exp(-t/\tau)$ for the decay] fits the data at shorter times [see Fig. 3(b)], with a relaxation time (both rise and decay) very close to $\tau_0$. The above photocurrent response is very similar to that measured when charging (or discharging) a capacitor ($C_p$) in series with a resistance ($R$), with a characteristic relaxation time $\tau_0 \cong (RC_p)$. Using a resistance value of $R \sim 120$ MΩ, deduced from the $I-V$ data (at 2 V), we extract a capacitance $C_p \sim 0.5$ nF.

In order to confirm the above picture, we carried out measurements of the photocurrent and voltage responses for a single layer device, where the pPPV was alternatively adsorbed with $C_{60}$. The behavior was substantially different from what was reported above. The open circuit voltage response was negligible, whereas the photocurrent measured had a finite initial value, but decayed rapidly to zero while the sample was still exposed to the laser beam. The $I-V$ characteristics were the same with and without laser exposure. The dark current data did not show a rectifying behavior as observed for the two-layer devices.

We now provide a discussion of the experimental results. The features shown in Figs. 1 and 2 indicate that upon exposure to the laser beam, photo carriers are generated at the interface between the PPV and $C_{60}$. Rapid electron transfer from the PPV to $C_{60}$ takes place.[4–6,11] This photoinduced electron transfer between the PPV and $C_{60}$ is at the origin of the measured photocurrent. Larger photocurrents are measured when the laser power is increased, or when higher energy photons are used (see Fig. 2). This is due to higher rates of photoinduced electron transfer when the laser power or the photon energy is increased. The effects of photon absorption by the PPV layer are negligible, e.g., Abs (at $\lambda=488$ nm and $\lambda=514$ nm)$\sim$0 whereas Abs ($\lambda=457$ nm)$\sim$0.03. The above photoinduced electron transfer also contributes to the substantial increase (by $\sim$two orders of magnitude) in the current flow through the device in comparison with the dark current.

The parallel drawn between the time dependence of the photocurrent resulting from a modulated laser irradiation (shown in Fig. 3) and the process of charging (or discharging) a capacitor in series with a resistance are also consistent with a photoinduced electron transfer. The charging of the capacitor when the cell is exposed to a laser beam results from carrier buildup on both sides of the heterojunction as electrons are transferred from the PPV to $C_{60}$, leaving holes behind across the interface. The current decay, once the beam is turned off, is due to carrier redistribution and flow through the device. This model has a few approximations, e.g., it does not take into account the fact that the interface is not smooth. Previous experiments showed that a surface heterogeneity of $\sim$10–30 Å characterizes the surface of thin films built using the present technique.[15]

The two transient features (dip and spike) in the photocurrent shown in Fig. 3 can also be attributed to carrier rearrangement at the heterojunction (capacitor). For instance, when the laser power is turned off, an additional short burst of carriers freed from the capacitor superposes on the value $I_0$, manifesting in the measured spike. The current then relaxes following the features shown in Fig. 3(b). Similarly, when the power is turned on, a very fast carrier rearrangement takes place near (or at) the interface to counterbalance the burst of charges created by the laser flux, which translates into a dip in the photocurrent. A single layer made of mixed PPV and $C_{60}$ does not present a heterojunction, and thus would not permit a macroscopic build up of photo induced charge transfer. This results in the features measured above, namely $\Delta V=0$ and very small photocurrents. The power efficiency of the present devices is $\sim 10^{-2}\%-10^{-3}\%$. It is lower than what was reported for the heterostructure of MEH–PPV.[4] This can be improved, for instance, by using higher density of PPV and $C_{60}$ per bilayer, along with other types of polycations.

The above set of data demonstrated that a heterostructure made of PPV/$C_{60}$ built using the simple and versatile technique of layer-by-layer sequential adsorption forms a rectifying and sensitive heterojunction. The present heterojunctions have the potential for use as sensitive solar cells with low dark currents and high open circuit voltages. Furthermore, because of the versatility of the present processing approach, larger area devices with various architectures and structures controllable at the microscopic scale can be made. Additional studies that take advantage of this approach to explore various architectures and use various polymers could give further insight into the understanding of the process of charge transfer between conjugated polymers and $C_{60}$.

This research was funded in part by NSF Grant No. DMR-91-57491, the NSF-MRSEC Program No. (DMR-94-00034), the Office of Naval Research, and the MURI Program of the Office of Naval Research.

[1] N. S. Sariciftci, L. Smilowitz, A. J. Heeger, and F. Wudl, Science **258**, 1474 (1992).
[2] N. S. Sariciftci, L. Smilowitz, D. Braun, G. Srdanov, V. I. Srdanov, F. Wudl, and A. J. Heeger, Synth. Met. **56**, 3125 (1993).
[3] L. Smilowitz, N. S. Sariciftci, R. Wu, C. Gettinger, A. J. Heeger, and F. Wudl, Phys. Rev. B **47**, 13835 (1993).
[4] N. S. Saricifci, D. Braun, C. Zhang, V. I. Srdanov, A. J. Heeger, G. Stucky, and F. Wudl, Appl. Phys. Lett. **62**, 585 (1993).
[5] S. C. Veenstra, G. G. Malliaras, H. J. Brouwer, F. J. Esselink, V. V. Krasnikov, P. F. vanHutten, J. Wildeman, H. T. Jonkman, G. A. Sawatzky, and G. Hadziioannou, Synth. Met. **84**, 971 (1997).
[6] G. Ruani, V. Dediu, M. Liess, E. Lunedei, R. Michel, M. Muccini, M. Murgia, C. Taliani, and R. Zamboni, Synth. Met. **103**, 2392 (1999).
[7] A. C. Fou, O. Onitsuka, M. Ferreira, M. F. Rubner, and B. R. Hsieh, J. Appl. Phys. **79**, 7501 (1996).
[8] H. Mattoussi, L. H. Radzilowski, B. O. Dabbousi, E. L. Thomas, M. G. Bawendi, and M. F. Rubner, J. Appl. Phys. **83**, 7965 (1998).
[9] H. Mattoussi, L. H. Radzilowski, B. O. Dabbousi, D. E. Fogg, R. R. Schrock, E. L. Thomas, M. F. Rubner, and M. G. Bawendi, J. Appl. Phys. **86**, 4390 (1999).
[10] A. Wu, D. Yoo, J.-K. Lee, and M. F. Rubner, J. Am. Chem. Soc. **121**, 4883 (1999).
[11] Y. Chi, J. B. Bhonsle, T. Canteenwala, J.-P. Huang, J. Shiea, B.-J. Chen, and L. Y. Chiang, Chem. Lett. **5**, 465 (1998).
[12] H. Mattoussi, F. E. Karasz, and K. H. Langley, J. Chem. Phys. **93**, 3593 (1990).
[13] H. Mattoussi, S. O'Donohue, and F. E. Karasz, Macromolecules **25**, 743 (1992).
[14] K. Hutchison, J. Gao, G. Schick, Y. Rubin, F. Wudl, J. Am. Chem. Soc. **121**, 5611 (1999).
[15] G. J. Kellogg, A. M. Mayes, W. B. Stockton, M. Ferreira, M. F. Rubner, and S. K. Satija, Langmuir **12**, 5109 (1996).